Supported by: Federal Ministry of Economics and Technology on the basis of a decision by the German Bundestag

Benefits of Receiver Clock Modeling in GNSS Navigation

Thomas Krawinkel and Steffen Schön
Institut für Erdmessung | Leibniz Universität Hannover | Germany

Introduction

Global Navigation Satellite Systems (GNSS) are one-way ranging systems. Consequently, receiver and satellites time scales have to be synchronized. This is generally realized by introducing satellite and receiver clock errors w.r.t. GNSS system time. Corrections for the satellite clock errors are broadcasted by the system provider, e.g. via GNSS navigation message. In contrast, due to the limited long-term frequency stability of the receiver's internal quartz oscillator and its generally poor accuracy, the receiver clock error has to be estimated epoch-by-epoch. This leads to (elevation-dependent) high mathematical correlations of 83–99% between the height component and the clock parameters (Fig. 1). As one consequence, the station height is typically determined about three times worse than the horizontal coordinates.

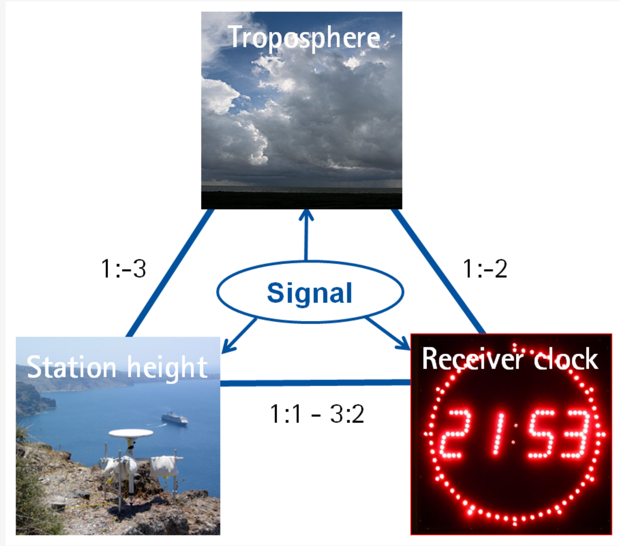

Fig. 1: Relationship between the parameters tropospheric delay, station height, and receiver clock error

This situation can be improved when using more stable clocks and modeling their behavior in a physically meaningful way instead of epoch-wise estimation. Especially kinematic Single Point Positioning (SPP) will benefit from such an approach called receiver clock modeling (RCM, Weinbach 2013). Recent developments of low-priced, low power consuming ($<$120 mW) miniaturized atomic clocks (MACs), primarily Chip Scale Atomic Clocks (CSACs), allow for usage in kinematic GNSS applications. Thus, replacing the receiver's internal oscillator by one of these much more stable external frequency standards opens up the possibility of RCM, and thereby improved positioning.

Clock Characterization

In order to correctly model the behavior of an external frequency standard in GNSS data analysis its stability has to be known. For the present study we use three different miniaturized atomic clocks: Jackson Labs LN CSAC, Microsemi Quantum™ SA.45s CSAC, and Stanford Research System PRS10.

At Physikalisch-Technische Bundesanstalt (PTB), these devices' 10 MHz output signals were compared to the phase of an active hydrogen maser (VREMYA-CH VCH-1003A) by means of a phase comparator with a selectable sampling interval of 1 s or 100 s.

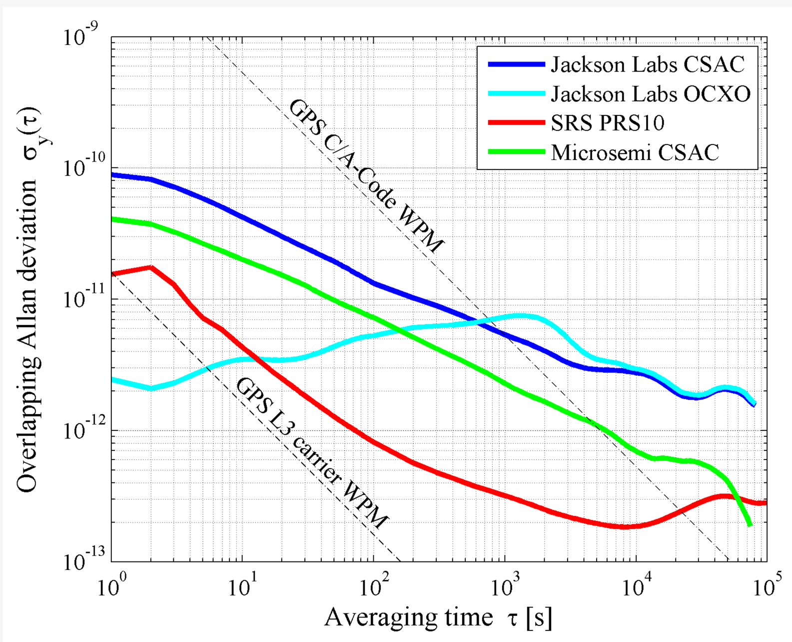

Fig. 2: Overlapping Allan Deviations

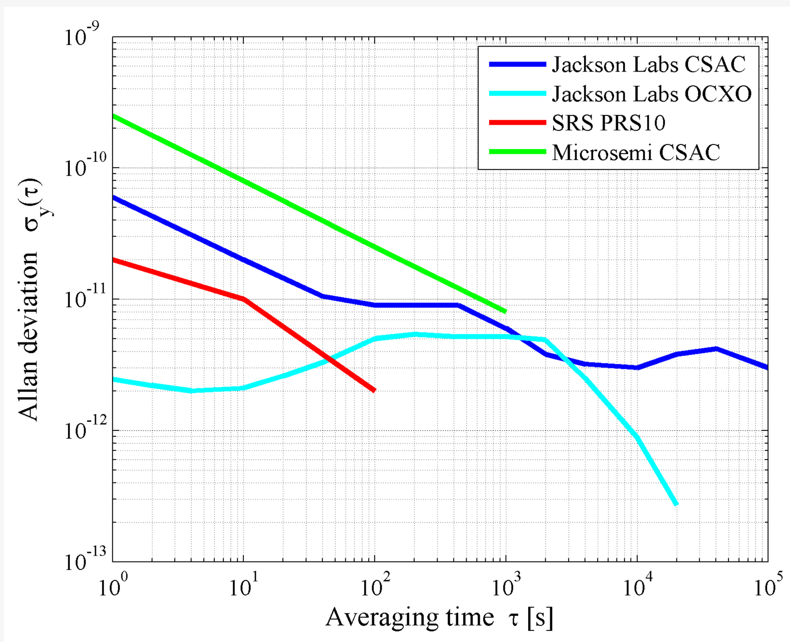

Fig. 3: Manufacturer's Allan Deviations

Jackson Labs LN CSAC

- CSAC: White Noise FM up to ca. 1 hour, then Flicker Noise FM
- CSAC: WFM 1.5 times worse than manufacturer's data
- OCXO: Typical high short-term stability, performance comparable to manufacturer's data
- RCM (C/A-code): $\tau \leq 12$ min.

Microsemi CSAC

- Similar noise types like JL CSAC, but ADEV about 5E-11 smaller
- Performance more than 5 times better than manufacturer's data
- Flicker Floor (FFM) after roughly three hours
- RCM (C/A-code): $\tau \leq 83$ min.

SRS PRS10

- Fluent passages of noise types
- White Noise PM to FM after approx. 15–20 s
- Short period of FFM around $\tau = 2$ hours, followed by Random Walk FM
- RCM (C/A-code): $\tau \leq 5.5$ hours

Kinematic Experiment

Data Acquisition

We carried out a real kinematic experiment on an eight-shaped cart-road in an approx. $500 \times 800\,\text{m}^2$ area with only a few natural obstructions in form of an alley (Fig. 5). The basic measurement configuration consisted of five *JAVAD Delta TRE-G3T(H)* receivers running an identical firmware version (3.4.14), and connected to one *NovAtel 703GGG* antenna via an active signal splitter. Four of these receivers were fed by the 10 MHz signals of our three MACs. For comparison reasons the fifth receiver was run by its internal oscillator.

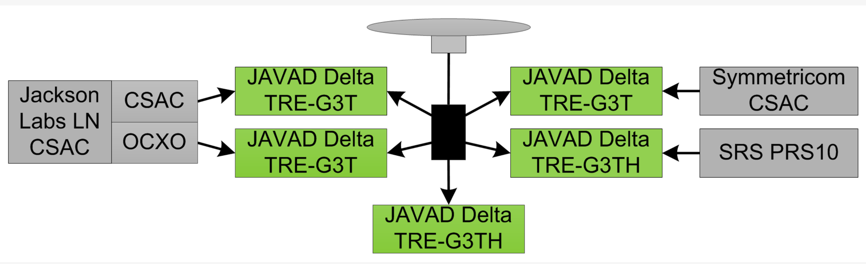

Fig. 4: Measurement configuration

Fig. 5: Test track with an expansion of ca. $500 \times 800\,\text{m}^2$; the yellow ellipse marks an alley with signal obstructions (source: Google Earth)

Concepts of Receiver Clock Modeling

One prerequisite for receiver clock modeling is that the clock noise has to be well below the GNSS receiver noise, i.e. the integrated random frequency fluctuations of the MACs cannot be resolved by the GNSS observations in use (Fig. 2). We assume typical values for code and ionosphere-free carrier phase observations of 1 m and 5 mm, respectively. Since these observations are phase-based measures, we can model the dominating underlying noise process as WPM over time. The intersection points between the dashed GPS observation noise lines and the ADEV curves define maximal time intervals for physically meaningful receiver clock modeling in our case study.

We compute two different real-time applicable navigation solutions:

- Modeling the process noise in an extended Kalman filter (EKF) using h_α-coefficients derived from ADEV in a model proposed by van Dierendonck et al. (1984)
- Applying a linear or quadratic (depending on the clock in use) clock polynomial in a sequential least-squares adjustment (SLSA)

Performance Analyses

Precision and Accuracy

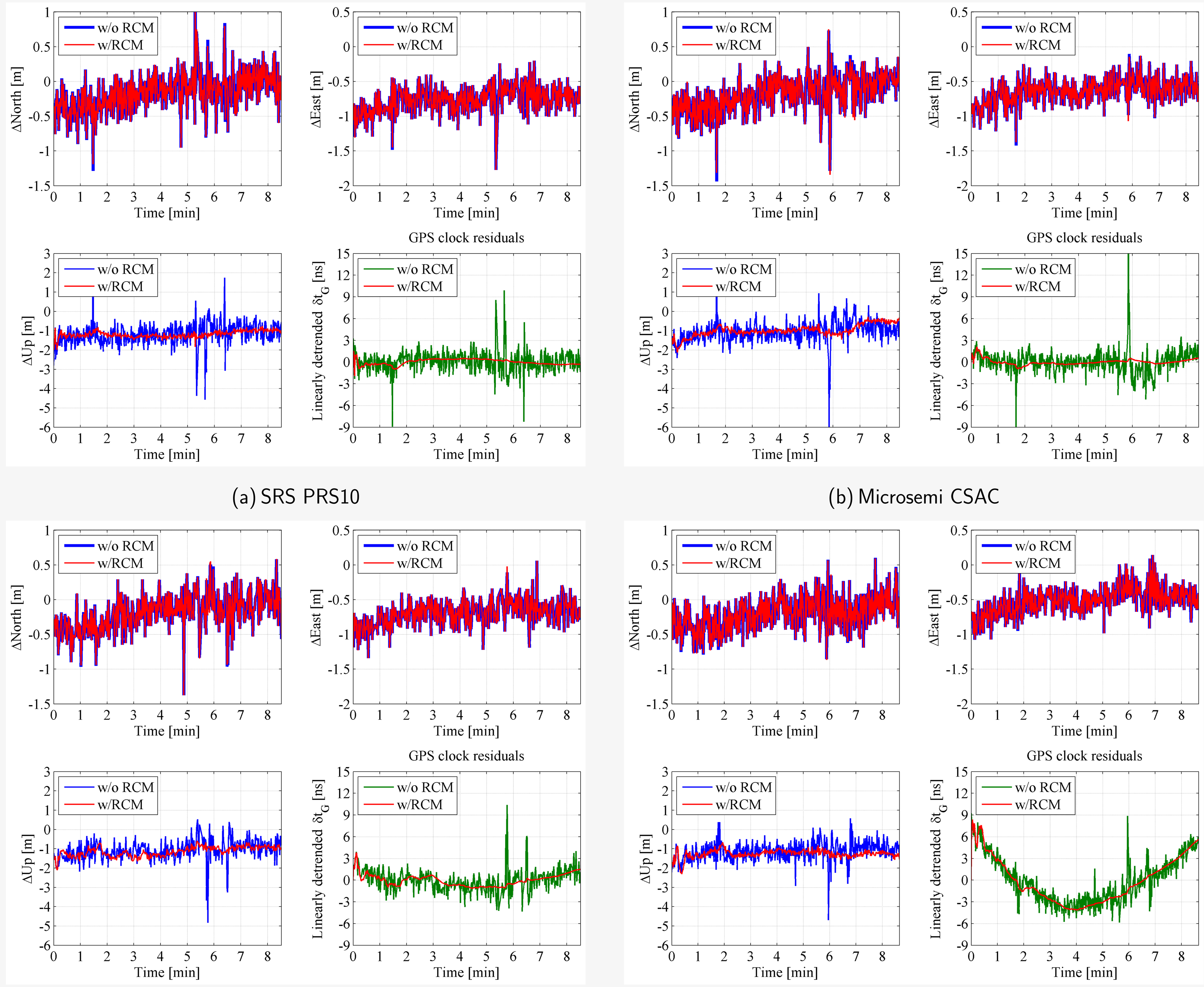

(a) SRS PRS10 (b) Microsemi CSAC

(c) Jackson Labs OCXO (d) Jackson Labs CSAC

Fig. 6: Topocentric coordinate deviations w.r.t. reference trajectory and clock errors after straight line fit. The results without receiver clock modeling are depicted in blue and green. The results when applying a polynomial for clock modeling in a sequential least-squares adjustment are shown in red. Note that in (a) and (b) linear polynomials, and in (c) and (d) quadratic polynomials are applied.

- Receiver clock modeling
  - leads to decreased clock estimates and smaller deviations of the up-coordinates from the reference solution (SRS PRS10 69% , Microsemi CSAC 48%, JL OCXO 53%, JL CSAC 58%)
  - has no effects on horizontal coordinates

Reliability

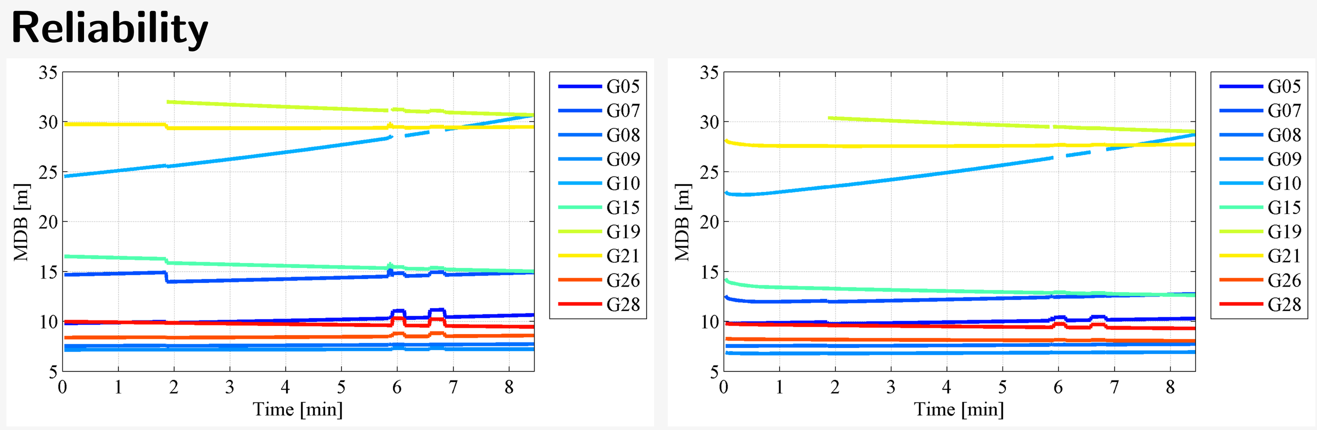

Fig. 7: Internal reliability of C/A-code observations in terms of minimal detectable bias (MDB) from receiver connected to the Microsemi CSAC: (left) values obtained without receiver clock modeling, (right) improved values when clock modeling is applied

- Max. improvement of 16.5% for G15 (mean MDB: 15.6 m → 13.0 m)
- MDB jumps for G10 when passing through the alley (signal interruptions) are also reduced

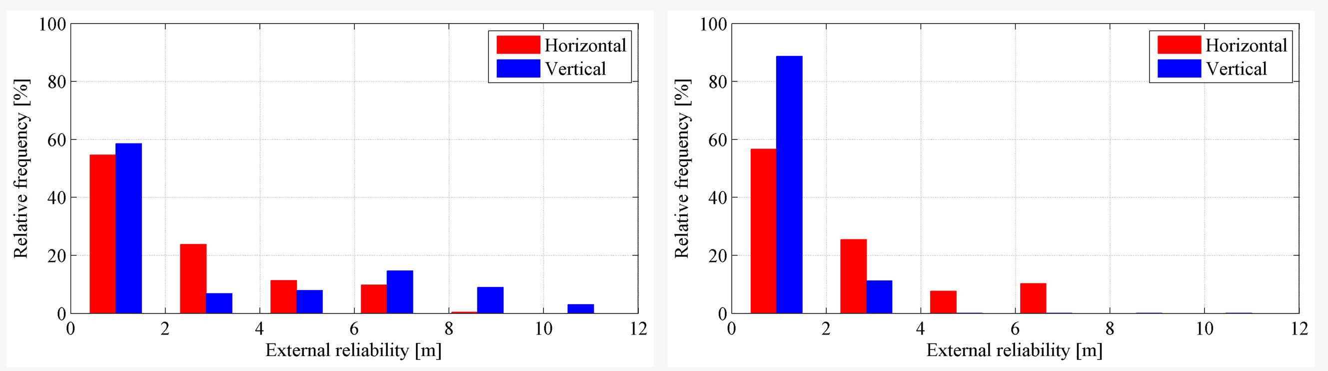

Fig. 8: Relative frequency of external reliability of horizontal and vertical coordinate components from the receiver connected to the Microsemi CSAC: (left) without, and (right) with receiver clock modeling

- No vertical values greater than 4 m remain (w/o RCM: 35%)
- Number of values smaller than 2 m increases (59% → 89%)

Availability and Continuity

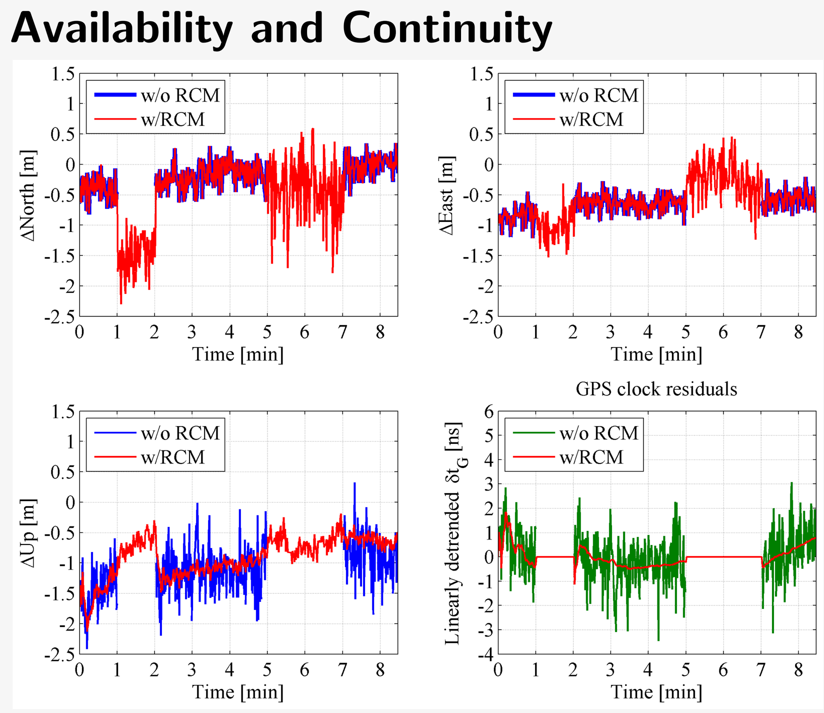

Fig. 9: Topocentric coordinate deviations w.r.t. reference trajectory, and clock errors after straight line fit. The receiver is connected to the Microsemi CSAC

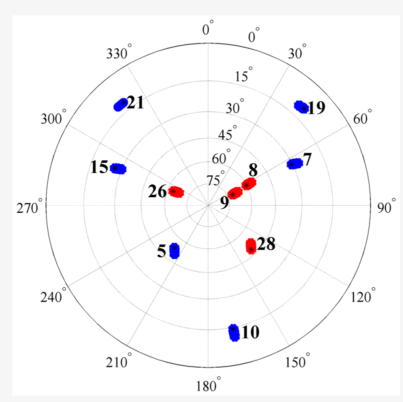

Fig. 10: Skyplot of satellite visibilities; only the satellites color-coded in red are used for clock coasting

- Generating two artifical partial satellite outages like, e.g., in urban environments
- Positioning with only three satellites possible due to known receiver clock behavior
- Additional correction in observation equation based on latest receiver clock coefficients

Conclusions

- Stability analyses of miniaturized atomic clocks show good agreement with manufacturer's data
- Benefits of receiver clock modeling:
  - Enhancing precision of up-coordinate by approx. 50%
  - Increasing estimation robustness
  - Improving availability and extending continuity in harsh environments

References

Krawinkel T, Schön S (2014) Applying Miniaturized Atomic Clocks for Improved Kinematic GNSS Single Point Positioning. Proceedings of the 27th International Technical Meeting of the Satellite Division of The Institute of Navigation (ION GNSS+), Tampa, FL, pp. 2431-2439

van Dierendonck A, McGraw J, Brown R (1984) Relationship Between Allan Variances and Kalman Filter Parameters. Proceedings of the Sixteenth Annual Precise Time and Time Interval (PTTI) Applications and Planning Meeting, Greenbelt, MD, pp. 273-293

Weinbach U (2013) Feasibility and impact of receiver clock modeling in precise GPS data analysis. Wissenschaftliche Arbeiten der Fachrichtung Geodäsie und Geoinformatik der Leibniz Universität Hannover, no. 303, PhD thesis

Institut für Erdmessung
Schneiderberg 50
D-30167 Hannover

26th General Assembly 2015 | International Union of Geodesy and Geophysics | Prague
June 22 – July 2, 2015

Thomas Krawinkel, Steffen Schön
www.ife.uni-hannover.de
{krawinkel, schoen}@ife.uni-hannover.de